

Magnetism of zigzag edge phosphorene nanoribbons

Zhili Zhu, Chong Li, Weiyang Yu, Dahu Chang, Qiang Sun, and Yu Jia

Citation: [Applied Physics Letters](#) **105**, 113105 (2014); doi: 10.1063/1.4895924

View online: <http://dx.doi.org/10.1063/1.4895924>

View Table of Contents: <http://scitation.aip.org/content/aip/journal/apl/105/11?ver=pdfcov>

Published by the [AIP Publishing](#)

Articles you may be interested in

[Electronic structure and magnetic properties of zigzag blue phosphorene nanoribbons](#)

J. Appl. Phys. **118**, 054301 (2015); 10.1063/1.4927848

[Tuning magnetic splitting of zigzag graphene nanoribbons by edge functionalization with hydroxyl groups](#)

J. Appl. Phys. **117**, 113902 (2015); 10.1063/1.4915337

[Transport properties of bare and hydrogenated zigzag silicene nanoribbons: Negative differential resistances and perfect spin-filtering effects](#)

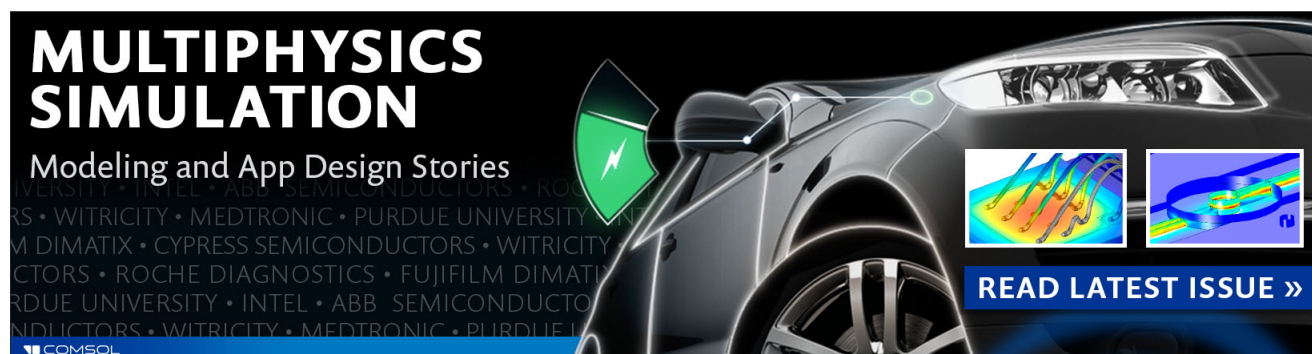
J. Appl. Phys. **116**, 124312 (2014); 10.1063/1.4896630

[Effects of edge hydrogenation on structural stability, electronic, and magnetic properties of WS₂ nanoribbons](#)

J. Appl. Phys. **114**, 213701 (2013); 10.1063/1.4829664

[Mechanically tunable magnetism on graphene nanoribbon adsorbed SiO₂ surface](#)

J. Appl. Phys. **111**, 074317 (2012); 10.1063/1.3702877

The advertisement for COMSOL Multiphysics Simulation features a dark background with a high-speed car on the right. On the left, the text 'MULTIPHYSICS SIMULATION' is in large, bold, white letters, followed by 'Modeling and App Design Stories' in a smaller white font. Below this, a list of partner companies is displayed in a very small, light blue font: 'UNIVERSITY • INTEL • ABB SEMICONDUCTORS • ROCHER • WITRICITY • MEDTRONIC • PURDUE UNIVERSITY • DIMATIX • CYPRESS SEMICONDUCTORS • WITRICITY • ROCHER DIAGNOSTICS • FUJIFILM DIMATIX • PURDUE UNIVERSITY • INTEL • ABB SEMICONDUCTORS • WITRICITY • MEDTRONIC • PURDUE UNIVERSITY'. A green shield icon with a white lightning bolt is positioned near the car. Two small inset images show simulation results: a heat map of a car engine and a 3D model of a car's aerodynamic flow. At the bottom right, a blue button with white text reads 'READ LATEST ISSUE »'. The COMSOL logo is in the bottom left corner.

Magnetism of zigzag edge phosphorene nanoribbons

Zhili Zhu,^{a)} Chong Li, Weiyang Yu, Dahu Chang, Qiang Sun, and Yu Jia^{a)}

International Joint Research Laboratory for Quantum Functional Materials of Henan, and School of Physics and Engineering, Zhengzhou University, Zhengzhou 450001, China

(Received 2 July 2014; accepted 4 September 2014; published online 17 September 2014)

We have investigated, by means of *ab initio* calculations, the electronic and magnetic structures of zigzag edge phosphorene nanoribbons (ZPNRs) with various widths. The stable magnetic state was found in pristine ZPNRs by allowing the systems to be spin-polarized. **The ground state of pristine ZPNRs prefers ferromagnetic order in the same edge but antiferromagnetic order between two opposite edges.** The magnetism arises from the dangling bond states as well as edge localized π -orbital states. The presence of a dangling bond is crucial to the formation of the magnetism of ZPNRs. **The hydrogenated ZPNRs get nonmagnetic semiconductors with a direct band gap. While, the O-saturated ZPNRs show magnetic ground states due to the weak P-O bond in the ribbon plane between the p_z -orbitals of the edge O and P atoms.** © 2014 AIP Publishing LLC.
[\[http://dx.doi.org/10.1063/1.4895924\]](http://dx.doi.org/10.1063/1.4895924)

Two dimensional (2D) layered crystal materials with atomic thickness have attracted extensive attention in recent years, such as graphene^{1,2} and molybdenum disulfide,³ due to their potential applications in future electronics. Most recently, a 2D few-layer black phosphorus or phosphorene^{4–7} has been fabricated by exfoliation. Phosphorene shows a finite direct band gap which can be modified from 1.51 eV for a monolayer to 0.59 eV for a five layer.⁸ It possess great transport properties such as high carrier mobility up to 1000 cm²/V·s which makes phosphorene a potential candidate for future nanoelectronic applications.⁹

For the phosphorene nanoribbons (PNRs), the edges of the ribbons play a critical role on their electronic properties. Guo *et al.*¹⁰ found that the pristine zigzag-PNRs (ZPNRs) are metals regardless of the ribbon width, while the pristine armchair-PNRs (APNRs) are semiconductors with indirect band gaps. Peng *et al.*¹¹ studied the edge effects and quantum confinement on the electronic properties of the PNRs with the edge functionalized using different chemical groups. They reported that the APNRs are semiconductors for all edge groups, and the ZPNRs demonstrate either semiconducting or metallic behavior.

We notice that all studies on the edge effects of PNRs reported in literatures did not concern with the magnetism. It is now well-known that the peculiar localized electronic states at each zigzag edge in graphene nanoribbons (GNRs) result in the spin polarization and half-metallicity.^{12,13} However, whether there exists intrinsic magnetism originated from edges in PNRs and how does it affect the properties of PNRs is an open question. Thus, in this letter, we have investigated the magnetic properties of ZPNRs by using first-principles calculations. The stable magnetic state was found in pristine ZPNRs by allowing the systems to be spin polarized. It was shown to have an indirect band gap instead of metallicity, with ferromagnetically ordered edge states at each edge but with the opposite spin directions between the

edges. The magnetism originated from edge states vanished when the dangling bonds at the zigzag edges were removed by H termination. While, the ZPNRs with O saturated edges were spin polarized, showing a ferromagnetic (FM) order in the same edge but antiferromagnetic (AFM) order between two opposites.

All calculations are performed by using Vienna *ab initio* simulation package (VASP) code¹⁴ based on density functional theory (DFT).¹⁵ The Perdew-Burke-Ernzerhof (PBE) exchange-correlation functional¹⁶ and the projector-augmented wave (PAW) potentials^{17,18} were employed. The kinetic energy cutoff for the plane wave basis set was chosen to be 500 eV. $20 \times 1 \times 1$ k-point meshes are used for the Brillouin zone integration for ZPNRs. A unit cell with periodic boundary condition was used to simulate a ribbon. A vacuum space of at least 12 Å was included in the unit cell to eliminate the coupling between neighboring cells. **The saturated atoms of both edges are fully relaxed until the force on each atom less than 0.01 eV/Å, with fixed pristine ZPNRs.**

The relaxed lattice constants for monolayer phosphorene are $a = 3.295$ Å, $b = 4.618$ Å which are good agreement with other theoretical calculations.^{10,11} We first explore the electronic and magnetic properties of pristine ZPNRs with width $nL = 12$ –28. The width of a ribbon nL is referred

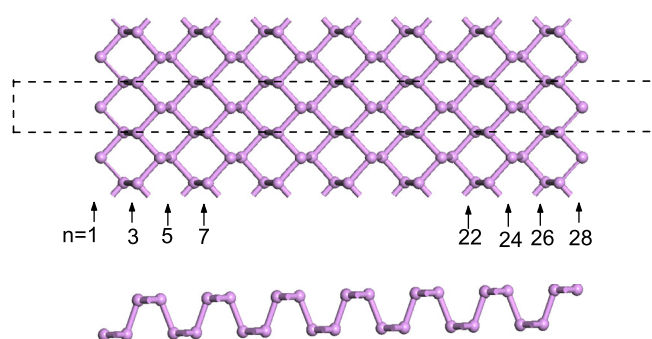


FIG. 1. Top and side views of structure of ZPNRs. The dashed rectangle indicates the unit cell.

^{a)}Authors to whom correspondence should be addressed. Electronic addresses: zlzhu@zzu.edu.cn and jiayu@zzu.edu.cn

according to the number n of P atoms in the direction perpendicular to the ribbon direction (see Fig. 1). The total energies of paramagnetic (PM), ferromagnetic (FM), and antiferromagnetic (AFM) orders were calculated, respectively. It was found that the stable magnetic states could be achieved by allowing the system to be spin polarized. Both the AFM and FM configurations are in energy lower than that of PM states for any width of the ribbons, indicating that spin polarization is a possible stabilization mechanism. Moreover, the AFM state which is FM coupling in the same zigzag edges but AFM between the two opposites has the lowest total energy among various spin configurations.

Fig. 2(a) shows the total energies of FM and AFM states as well as the energy difference $E_{\text{FM}} - E_{\text{AFM}}$ per unit cell for $n\text{L-ZPNR}$. One can see that the AFM state is energetically more favorable than the FM state by 18 meV for 12L-ZPNR. And, the energy difference between the FM and AFM spin configurations decreases as $n\text{L}$ increases and almost vanishes for $n=28$. It is beyond the decay length of the spin polarization at the two edges when the width is larger than $n\text{L}=28$. Similar case in pristine ZGNRs was also found.^{19,20}

To give a further insight of the magnetism of pristine ZPNRs, we have calculated the spin densities of FM and AFM spin configurations for different ribbon widths. Fig. 2(b) shows one case of AFM states for $n\text{L}=20$. It is found that the total magnetic moment is mainly contributed by edge atoms and their adjacent atoms with total magnetic moment of $m=1.0 \mu_B$ in a unit cell for each edge. The edge P atom and its nearest and next nearest neighbors contribute to the local magnetic moments in a unit cell of 0.65, 0.12, and $0.11 \mu_B$, respectively.

To better understand the effects of edge magnetism on the electronic properties of ZPNRs, the band structures of PM, FM, and AFM states corresponding to different ribbon widths were calculated, respectively. As an example, Fig.

2(c) demonstrates the computed electronic structure of the 20L-ZPNR. The partial charge density distribution shows that the two bands across the Fermi level which result in metallic character of PM state stem from the P atoms near the edges. In the spin polarized FM state, the up and down channels of α , β bands are pushed away from the Fermi level to higher and lower energies. The up bands are occupied, while down bands are empty, leading to an indirect band gap but very small. In the AFM state, the α and β bands are split just above and below the Fermi level, resulting in a band gap larger than that of FM state. Moreover, It was found that the PM state is metallic regardless of the ribbon width from $n=12$ to 28 which is consistent with literature.⁹ However, both the AFM and FM states demonstrate semiconductor with finite indirect band gaps depending on the ribbon width. Fig. 2(d) presents the width dependence of band gaps of the semiconducting ZPNRs. It shows that the band gap of AFM state increases with a reduced width of the ribbon. While, it decreases with the reduced ribbon width for FM state, i.e., it decreases from 0.09 eV for 28L-ZPNR to 0.04 eV for 20L-ZPNR, and becomes a semiconductor with a zero band gap for 12–16L-ZPNRs. This trend may be explained by the following understanding: As for a certain width of pristine ZPNR, its ground state prefers AFM order between two opposite edges with a larger band gap than that of FM state. The spin coupling of two edges will be strengthened with a reduced width of the ribbon. Meanwhile, the FM state gets more unstable relative to the ground AFM state, and the band gap undergoes a reverse trend to that of AFM state.

In order to probe more detailed features of the edge magnetism, the electronic and magnetic properties of ZPNRs with edges saturated with H and O atoms were studied, respectively. It was found that the magnetism vanished in the hydrogen-saturated nanoribbon. It becomes a direct-gap semiconductor, and its band gap is a strong function of the

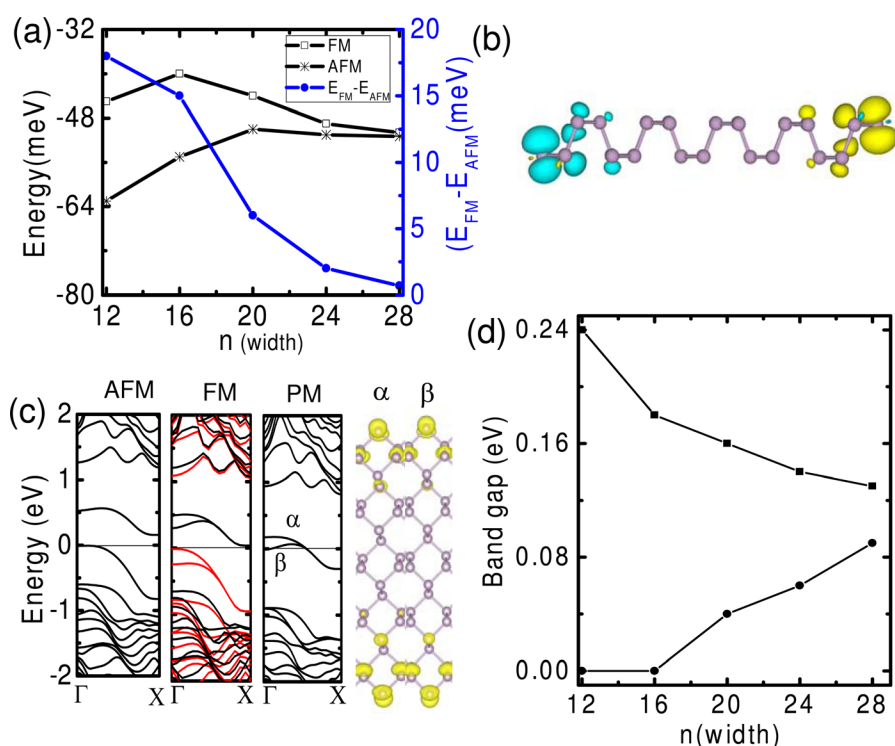


FIG. 2. (a) Total energies of FM and AFM with respect to PM phase as well as the energy difference ($\Delta E = E_{\text{FM}} - E_{\text{AFM}}$) as a function of the ribbon width for pristine ZPNRs, denoted here by the index n . (b) Side view of spin density ($\rho_{\text{up}}, \rho_{\text{down}}$) of 20L-ZGNR in the AFM state. Yellow and cyan indicate the positive and negative densities, respectively. The isosurface value is $0.004 \text{ e}/\text{\AA}^3$. (c) Computed band structures of 20L-ZGNR in the AFM, FM, and PM states, respectively. Right panels show the partial charge density distribution of the corresponding α and β bands of PM state. The isosurface value is $0.004 \text{ e}/\text{\AA}^3$. (d) Band gaps of AFM and FM states depending on the ribbon width.

ribbon width due to quantum confinement effect. So, it can be concluded that the presence of a dangling bond is crucial to the formation of the magnetism of ZPNRs. The spin-density plot shown in Fig. 2(b) reveals the spatial distribution of both dangling bond states and the tails of the spin-polarized π -orbital states. It is obvious that the magnetic moment at the edge arises from both dangling bonds as well as edge localized π -orbital states. The dangling bond states localized at the edge contribute significantly to the total magnetic moment. And, the magnetism originated from edge atom induced the polarization of its adjacent atoms. If the dangling bond is saturated by H, the edge P atom has no magnetic moment anymore and the inducement which results in polarization of its adjacent atoms will vanish concomitantly. The gap states in pristine ZPNRs are removed after the H termination. The H-saturated ZPNRs are nonmagnetic semiconductors with a direct band gap.

However, the ZPNRs with O saturated edges were spin polarized, showing a FM order in the same edge but AFM order between two opposite edges which are similar with that of pristine ZPNRs. The optimized structure parameters are shown in Fig. 3(d). The O-P bond length is 1.51 Å, the P-P bond length at the edge is 2.23 Å, and the bond angle θ between O and the edge P atoms is 123.8°. As shown in Fig. 3(a), the AFM state is in energy lower than that of FM state in the oxygen-saturated nanoribbon. Similar with the case of pristine edge, the energy difference between the FM and AFM states decreases as the increased ribbon width. And, the total energies of FM and AFM states get degenerate when n is larger than 28.

The calculated band structures of the oxygen-saturated ZPNRs showed that the PM state is metallic regardless of the ribbon width, while the AFM and FM states are semiconductor. As one example, the electronic structure of the 20L-ZPNR with O-saturated edges was shown in Fig. 3(b).

The band gaps of AFM and FM states as a function of the ribbon width is shown in Fig. 3(c). Comparing with the case of pristine ZPNRs, the band gaps of oxygen-saturated ZPNRs are less sensitive to the changes of ribbon width. It was found that the decorated O atoms prefer same spin direction in the oxygen-saturated ZPNRs if the edge P atoms are

forbid to be spin polarized. So, the spin coupling of O atoms between two edges help to minish the energy difference between FM and AFM states in the oxygen-saturated ZPNRs. For this reason, the energy difference between FM and AFM states is a little smaller than that of pristine ZPNRs for a certain width of ribbon.

To give a detailed analysis of why oxygen-saturated ZPNRs are spin polarized while H-saturated edges not, the spin densities of oxygen-saturated nanoribbons have been calculated. From the spin densities of O-20L-ZPNR shown in Fig. 3(d), one can see that the magnetic moments mainly localize on the two zigzag edges contributed by O atoms as well as their adjacent P atoms. The local magnetic moments in a unit are $0.27 \mu_B$ for O atom, $0.39 \mu_B$ for edge P atom, and $0.13 \mu_B$ for its nearest neighbor, respectively.

We examined the characteristics of the electronic orbitals of the decorated O atoms and edge P atoms. It was found that the edge P atoms do not form a saturated bond with the decorated O atoms. As the right panels related with α and β bands shown in Fig. 3(b), the p_z -orbitals of the edge O and P atoms form a relatively weak P-O bond in the ribbon plane due to the a minimal overlap of the wavefunction. In consequence, these unsaturated bonds bring magnetic moments in oxygen-saturated ZPNRs.

Naturally, it is of great importance to evaluate the relative stabilities of the O-ZPNRs. We calculated the Gibbs free energies to investigate the stability of O-ZPNRs.²¹ For comparison, the stability of hydrogen-saturated ZPNRs was also studied. The stabilities of O- and H-ZPNRs with respect to pristine ZPNRs are plotted in Fig. 4. The calculated results reveal that O terminated ZPNRs are more stable than the bare case when the chemical potential of oxygen μ_O gradually approaches to O-rich condition, indicating that it is plausible to realize the O terminated ZPNRs. Furthermore, the O-ZPNRs has a larger stable range to be formed in experiment, i.e., $\mu_O > -5.27\text{eV}$ than H- ZPNRs, i.e., $\mu_H > -3.12\text{eV}$.

In this study, we focus on the intrinsic magnetism of bare and H-, O- terminated ZPNRs. The atoms of pristine ZPNRs are fixed in our calculations. If the structures are fully relaxed, the pristine ZPNRs will undergo Peierls

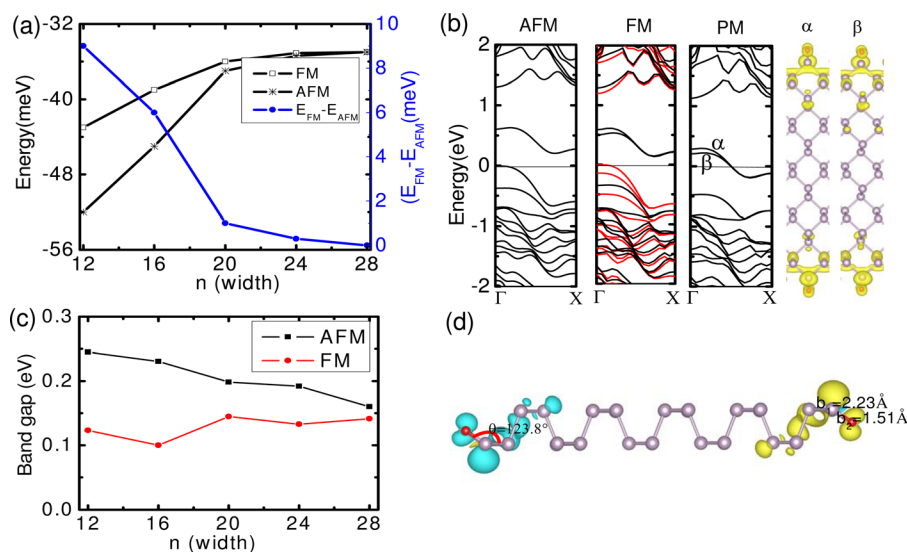


FIG. 3. (a) Total energies of FM and AFM with respect to PM phase as well as the energy differences between FM and AFM states varying with the ribbon width for oxygen-saturated ZPNRs. (b) Band structures of the 20L-ZPNR in the AFM, FM, and PM states, respectively. Right panels show the partial charge density distribution of the corresponding α and β bands for PM state. The isosurface value is $0.004 \text{ e}/\text{\AA}^3$. (c) Band gaps of the ribbon width for the AFM and FM states, respectively. (d) Side view of spin density ($\rho_{\text{up}} - \rho_{\text{down}}$) of 20L-ZPNR in the AFM state. Yellow and cyan indicate the positive and negative densities, respectively. The isosurface value is $0.004 \text{ e}/\text{\AA}^3$.

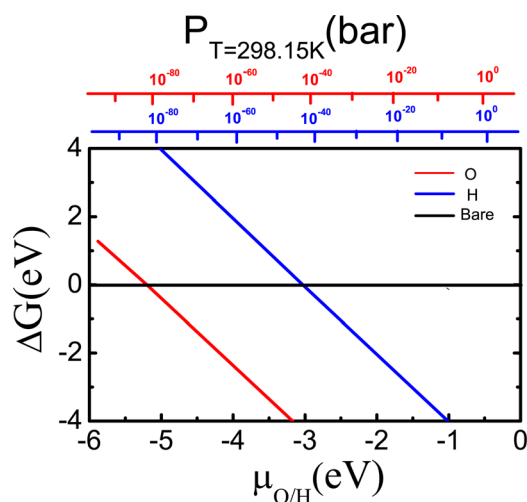


FIG. 4. The stability properties of O-ZPNRs and H-ZPNRs with respect to pristine ZPNRs.

transition leading to opening of a band gap in the electronic structure.²² In the fully relaxed O-ZPNRs, the bond lengths as well as bond angles at the edges will change due to the lattice distortion. The P-P bond length at the edge increases from 2.23 Å (shown in Fig. 3(d)) to 2.25 Å, while the bond angle θ between O and the edge P atoms decreases from 123.8° to 116.5°. It is worth noting that both Peierls distortion in pristine ZPNRs and edge reconstruction in O-ZPNRs can make the dangling bond saturated and lead to nonmagnetic phosphorene nanoribbons.

In summary, we have investigated the intrinsic magnetism originated from edges of ZPNRs. The spin polarized states are observed in pristine ZPNRs. It was found that the presence of a dangling bond is crucial to the formation of the magnetism of ZPNRs. The dangling bond states localized at the edges contribute significantly to the total magnetic moment. The hydrogenated ZPNRs get nonmagnetic since the dangling bond is saturated. However, the ZPNRs with the O saturated edges are spin polarized due to the weak P-O bond in the ribbon plane between the p_z -orbitals of the edge O and P atoms.

Z. L. Zhu and Y. Jia gratefully acknowledge financial supports from the National Basic Research Program of China (No. 2012CB921300). The calculations were performed on the High Performance Clusters of Zhengzhou University.

- ¹K. S. Novoselov, A. K. Geim, S. V. Morozov, D. Jiang, M. I. Katsnelson, I. V. Grigorieva, S. V. Dubonos, and A. A. Firsov, *Nature* **438**, 197 (2005).
- ²Y. B. Zhang, Y. W. Tan, H. L. Stormer, and P. Kim, *Nature* **438**, 201 (2005).
- ³B. Radisavljevic, A. Radenovic, J. Brivio, V. Giacometti, and A. Kis, *Nat. Nanotechnol.* **6**, 147 (2011).
- ⁴L. Li, Y. Yu, G. J. Ye, Q. Ge, X. Ou, H. Wu, D. Feng, X. H. Chen, and Y. Zhang, *Nat Nanotechnol.* **9**, 372 (2014).
- ⁵H. Liu, A. T. Neal, Z. Zhu, Z. Luo, X. Xu, D. Tománek, and P. D. Ye, *ACS Nano* **8**, 4033 (2014).
- ⁶F. Xia, H. Wang, and Y. Jia, *Nat. Commun.* **5**, 4458 (2014).
- ⁷E. S. Reich, *Nature* **506**, 19 (2014).
- ⁸J. Qiao, X. Kong, Z.-X. Hu, F. Yang, and W. Ji, *Nat. Commun.* **5**, 4475 (2014).
- ⁹M. Buscema, D. J. Groenendijk, S. I. Blanter, G. A. Steele, H. S. J. van der Zant, and A. Castellanos-Gomez, *Nano Lett.* **14**, 3347 (2014).
- ¹⁰H. Guo, N. Lu, J. Dai, X. Wu, and X. C. Zeng, *J. Phys. Chem. C* **118**, 14051 (2014).
- ¹¹X. Peng and Q. Wei, "Edge effects on the electronic properties of phosphorene nanoribbons," preprint [arXiv:1404.5995](https://arxiv.org/abs/1404.5995) (2014).
- ¹²Y.-W. Son, M. L. Cohen, and S. G. Louie, *Phys. Rev. Lett.* **97**, 216803 (2006).
- ¹³K. Nakada, M. Fujita, G. Dresselhaus, and M. S. Dresselhaus, *Phys. Rev. B* **54**, 17954 (1996).
- ¹⁴G. Kresse and J. Furthmüller, *Phys. Rev. B* **54**, 11169 (1996).
- ¹⁵W. Kohn and L. J. Sham, *Phys. Rev.* **140**, A1133 (1965).
- ¹⁶J. P. Perdew, K. Burke, and M. Ernzerhof, *Phys. Rev. Lett.* **77**, 3865 (1996).
- ¹⁷P. E. Blöchl, *Phys. Rev. B* **50**, 17953 (1994).
- ¹⁸G. Kresse and D. Joubert, *Phys. Rev. B* **59**, 1758 (1999).
- ¹⁹H. Lee, Y.-W. Son, N. Park, S. Han, and J. Yu, *Phys. Rev. B* **72**, 174431 (2005).
- ²⁰L. Pisani, J. A. Chan, B. Montanari, and N. M. Harrison, *Phys. Rev. B* **75**, 064418 (2007).
- ²¹The Gibbs free energies $G_O = \varepsilon_O - \mu_O$ was calculated to determine the stabilities of O-ZPNRs. ε_O is the formation energies defined as: $\varepsilon_O = E_{\text{total}} - n_P E_P - n_O E_O$, where E_{total} is the total energy of oxygen terminated O-ZPNRs, E_P and E_O are the energies of an isolated spin-polarized phosphorus and oxygen atom, respectively. μ_O is the chemical potential of oxygen which is the function of the temperature T and the partial oxygen atom pressure P with the definition of $\mu_O = H^0(T) - H^0(0) - TS^0(T) + K_B T \ln(P/P^0)$. The room temperature $T = 298.15\text{K}$ is considered. H^0 and S^0 are the enthalpy and entropy at the pressure of O content $P^0 = 1$ bar.
- ²²V. Tran and L. Yang, *Phys. Rev. B* **89**, 245407 (2014).